Enhanced Coherent BOTDA System Without Trace Averaging

Nan Guo, Liang Wang, *Member, IEEE, Member, OSA*, Huan Wu, Chao Jin, Hwa-Yaw Tam, *Fellow, OSA*, and Chao Lu, *Fellow, OSA*

***Abstract*—We propose and experimentally demonstrate a scheme of a coherent Brillouin time domain analysis (BOTDA) system without any trace averaging. Assisted by a commercial integrated coherent receiver with a local oscillator generated through single sideband modulation from the same laser source, the Brillouin signals carried on a stable intermediate frequency (IF) are extracted by electrical/digital filters and then recovered to baseband by digital signal processing. This increases the signal-to-noise ratio and avoids the need of trace averaging and enables real-time signal acquisition.To eliminate the Brillouin gain fluctuation, two adjacent Brillouin time-domain traces stimulated by two sequential orthogonal pump pulses are recovered after the IF signals are detected in a real-time manner. Based on this configuration, a spatial resolution of 4 m and Brillouin frequency shift uncertainty of 1.473 MHz are realized in distributed temperature sensing over 40.63 km range. With the nonlocal means algorithm and distributed Raman amplification integrated into the system, the BFS uncertainty is enhanced to 0.843 MHz and better spatial resolution of 2 m over the same sensing fiber is achieved.**

***Index Terms*—Brillouin optical time domain analyzer, Brillouin scattering, distributed sensing, fiber optics sensors.**

I. Introduction

As ONE of the most popular distributed optical fiber sensing (DOFS) systems, Brillouin time domain analysis (BOTDA) has been developed for nearly three decades, since it was first proposed and demonstrated [1]–[3]. In most of the BOTDA systems, by scanning the pump-probe frequency difference, the Brillouin gain spectrum (BGS) can be reconstructed to determine the distribution of Brillouin frequency shift (BFS) which can be mapped to the distributed temperature and/or strain information along the sensing fiber. The performance of a BOTDA system in terms of spatial resolution, sensing range, frequency uncertainty is limited by the signal-to-noise ratio (SNR) of the sensor response [4], and hence to improve the SNR becomes the main challenge for high-performance BOTDA. High SNR usually requires high input powers of the probe and pump lightwaves, which are not feasible since the peak power of the pump pulse is restricted by fiber nonlinearities [5], [6], and power of the probe lightwave is also limited to avoid the nonlocal effects [7].

To overcome the limitations mentioned above, a lot of efforts have been made in recent years [8]–[26], and many approaches have been proposed including optical coding [8], [9], Raman amplification [11]–[13], and image processing [19]. Among them, coherent detection is an attractive solution to enhance the SNR performance and to enable Brillouin phase detection [14]–[16]. In these coherent detection schemes, however, the optical local oscillator (LO) lightwave is generated together with the probe and injected into the fiber under test (FUT) at the same time to avoid the laser phase noise. The power of LO is limited due to the fiber nonlinearities. For applications with long sensing range, the insufficient LO power after transmission along the FUT will limit the performance of coherent detection since shot noise limited performance cannot be achieved. In order to solve this problem, an alternative scheme has been proposed and demonstrated using a separated laser as the LO together with a commercial coherent receiver to allow shot noise limited performance for better SNR performance of the detected signal [17]. It is also possible for phase detection if the coherent length of the lasers used is much longer than the length of the sensing fiber. At the same time, the scheme provides the advantage of using electrical/digital filtering and digital signal processing (DSP) to recover the sensing signal. Benefiting from this advantage, the system is able to get rid of the ultra-narrow optical bandpass filters at the receiver end. This is very useful for practical system applications considering that the precise alignment of the filter with the probe signal is often a very challenging task in practical BOTDA systems. However, the system performance is affected by the drift of relative frequency between the lasers, which lead to the instability of the intermediate frequency (IF) and hence a large number of trace averaging required to minimize the effect. Moreover, the data acquisition in [17] is time-consuming due to trace averaging. Another problem with all demonstrated schemes is polarization scrambling is always necessary to avoid

Manuscript received June 14, 2017; revised August 5, 2017 and August 13, 2017; accepted August 15, 2017. Date of publication August 20, 2017; date of current version February 24, 2018. This work was supported in part by the National Natural Science Foundation of China under Grant 61377093, in part by the Hong Kong RGC GRF grant (PolyU 5208/13E), and in part by the Project of The Hong Kong Polytechnic University (1-ZVFL). *(Corresponding author: Liang Wang.)*

N. Guo, C. Jin, and C. Lu are with the Department of Electronic and Information Engineering, The Hong Kong Polytechnic University, Kowloon, Hong Kong, and also with the Shenzhen Research Institute, The Hong Kong Polytechnic University (Shenzhen Base), Nanshan, China (e-mail: neil.nan.guo@outlook.com; jinchao1573@hotmail.com; chao.lu@polyu.edu.hk).

L. Wang and H. Wu are with the Department of Electrical Engineering, The Chinese University of Hong Kong, Shatin, Hong Kong (e-mail: lwang@ee.cuhk.edu.hk; hwu@ee.cuhk.edu.hk).

H.-Y. Tam is with the Department of Electrical Engineering, The Hong Kong Polytechnic University, Kowloon, Hong Kong (e-mail: hwa-yaw.tam@polyu.edu.hk).

Color versions of one or more of the figures in this paper are available online at http://ieeexplore.ieee.org.

Digital Object Identifier 10.1109/JLT.2017.2742598

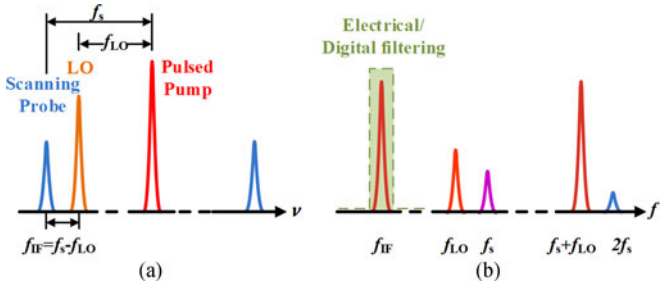

Fig. 1. (a) The frequency alignment of the pulsed pump, the dual-sideband probe, and the LO in our coherent-detection assisted BOTDA; (b) the frequency components at the output of coherent receiver before electrical filtering.

the effect of relative polarization change between pump and probe signals. Because of all these, single trace measurement is not possible and this has affected the use of the sensing scheme for practical high speed measurement.

Recently, we have demonstrated an enhanced configuration of coherent BOTDA over 40 km sensing range without trace averaging for real-time data acquisition. [27] In addition to the improved signal-to-noise ratio (SNR) from the use of a commercial integrated coherent receiver, the LO lightwave generated by single-sideband (SSB) modulation guarantees stable IF signals carrying the Brillouin sensing signals. The IF signals are extracted after electrical/digital filtering and measured with a real-time oscilloscope. To minimize polarization dependent fluctuation, two adjacent baseband Brillouin time-domain traces stimulated by pump pulse sequence with adjacent pulses orthogonal in polarization to each other are recovered and combined by digital signal processing (DSP). Benefiting from this configuration, the need of trace averaging is avoided and hence the data acquisition can be completed in a real-time mode. In this paper, we further extend the scheme to achieve better sensing performance. We show that using this proposed scheme with non-local means (NLM) algorithm and distributed Raman amplification, a BFS uncertainty of 0.843 MHz and spatial resolution of 4 m over the 40.63 km sensing fiber is achieved with no trace averaging applied. This is significantly better than the reported BOTDA schemes based on coherent detection.

The paper is organized as follows. Section II describes the principle of our coherent BOTDA with real-time data acquisition. The experiment setup is illustrated in this section. Section III presents the experiment results together with those of enhanced sensing performance by integrating the non-local means (NLM) algorithm and distributed Raman amplification into the system. Finally, the study is concluded in Section IV.

II. Principle and Experimental Setup

The principle of our coherent BOTDA is to use single-sideband modulated local oscillator (LO) light generated from the same laser source in a commercial phase- and polarization-diversity coherent receiver to enhance the reception of sensing signals and hence avoid the need of trace averaging for real-time data acquisition. In our scheme, the LO light is provided from the same light source of the BOTDA system with frequency down-shifted by *f*LO from the laser or pump frequency, as shown in Fig. 1(a). The probe light consists of two sideband components which are upshifted and downshifted by $f_{\rm s}$ from the pump frequency, respectively, and are frequency-scanned. The LO and probe light are injected into the respective port of an integrated coherent receiver simultaneously. The output electrical signals from the receiver are generated by beating of the optical waves in Fig. 1(a) and generated frequency components are shown in Fig. 1(b) where the one with a stable intermediate frequency of $f_{\rm IF} = f_{\rm s} - f_{\rm LO}$ carries the Brillouin gain information. By using electrical low-pass filtering and subsequent digital filtering, the frequency component at $f_{\rm IF}$, can be accurately and detected.

The detected signal after electrical filtering can be expressed as:

$$I \propto R\sqrt{\frac{P_{S0}\left(1+G_B(t)\right)P_{\rm LO}}{2}}\exp\left[j\left(2\pi f_{\rm IF}t+\varphi_{\rm LO}\right.\right.$$
$$\left.\left.-\varphi_B(t)+\varphi_N\right)\right]+{\rm c.c} \quad (1)$$

where *R* is the responsivity of the receiver, P_{S0}, $P_{\rm LO}$ are the input powers of the lower sideband probe and LO, $G_{\rm B}(t)$ and $\varphi_{\rm B}(t)$ are the Brillouin gain and induced phase, $\varphi_{\rm LO}$, and $\varphi_{\rm N}$ are the phase of LO and the phase noise between the LO and probe, respectively, and c.c means the complex conjugate of the signal. It can be seen from (1) that the amplitude of the IF signal is proportional to the Brillouin gain, and the powers of the probe and LO. Benefiting from a separate LO directly delivered into the receiver without propagation loss, the signal-to-noise ratio of the received signal will be greatly enhanced by the shot-noise limited receiver performance, compared to most of the previous coherent BOTDA schemes. Moreover, benefiting from the use of the SSB generated LO from the same laser source, the detected IF signals shall maintain as a stable frequency at each scanning frequency of the sensing system, which facilitates the electrical/digital filtering and the subsequent DSP for the recovery of the sensing signal within the baseband. The IF can easily be adjusted based on required dynamic range of the system.

In our experiment, as a commercial phase- and polarization-diversity coherent receiver is used for coherent detection, the in-phase ($I_{\rm x}$, $I_{\rm y}$) and quadrature-phase ($Q_{\rm x}$, $Q_{\rm y}$) components of the signal in (1) in both x, y polarizations are received simultaneously via the four outputs of the receiver. The four outputs are then processed using the digital signal processing (DSP) algorithms in this way: they are transformed into frequency domain by fast Fourier transform (FFT) and filtered by a subsequent digital bandpass filter designed with a center frequency exactly the same as the IF to remove most of the noise in frequency domain, and then transformed back to the time domain and combined to recover the baseband Brillouin time-domain traces based on the following relationship [17]:

$$P_S(t) \propto I_x^2 + Q_x^2 + I_y^2 + Q_y^2 \quad (2)$$

The signal in (2) contains the enhanced baseband Brillouin sensing signal without any trace averaging and is used to extract sensing information. To minimize the polarization dependent gain variation of Brillouin scattering for real-time data acquisition, adjacent pump pulses are made orthogonal in polarization to each other by using a polarization switch driven by level signals that are synchronized with the pump pulse generation at the same repetition rate, as shown in Fig. 2. As a result of this, two

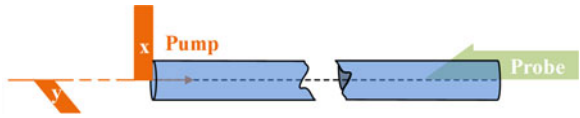

Fig. 2. The configuration of orthogonal pump pulse sequence at each scanning frequency to suppress polarization dependent fluctuation.

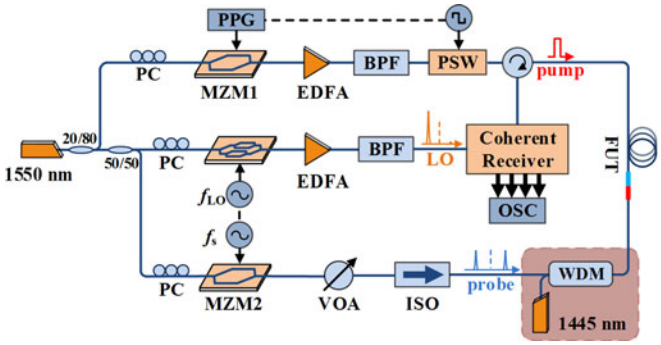

Fig. 3. Experiment setup of the coherent BOTDA without trace averaging. PC, polarization controller; EDFA, Erbium-doped fiber amplifier; BPF, band pass filter; MZM, Mach-Zehnder Modulator; PPG, pulse pattern generator; PSW, polarization switch; VOA, variable optical attenuator; ISO, isolator; OSC, Oscilloscope; FUT, fiber under test; WDM, wavelength division multiplexer. The components within the red region serve as extra Raman amplifier used for high spatial resolution experiment.

recovered adjacent Brillouin time-domain traces triggered by two sequential orthogonal pump pulses are utilized to minimize the polarization dependent fluctuation of Brillouin gain.

Fig. 3 shows the experiment setup of the coherent-detection assisted BOTDA system without trace averaging. The output light of a 1550 nm laser is split into three branches by 20/80 and 50/50 couplers, respectively. In the upper branch, a high-extinction-ratio Mach-Zehnder modulator (MZM1, 40 dB extinction ratio) and a pulse pattern generator (PPG) are employed to generate pump pulses. The erbium-doped fiber amplifier (EDFA) in the branch boosts the peak power of the pulses, and a bandpass filter with the bandwidth of 1 nm is used to reduce the amplified spontaneous emission (ASE) noise from the EDFA. Driven by a function generator which is synchronized with the PPG at the same repetition frequency as the pump pulses, a polarization switch (PSW) is used to make adjacent pump pulses orthogonal to each other, in order to minimize the polarization dependent gain fluctuation. Then the pump pulses are delivered to the FUT through a circulator. Operated in single-sideband (SSB) modulation mode, the IQ modulator in the middle branch together with a radio frequency (RF) synthesizer with fixed output frequency of 10 GHz are used to generate a lightwave as the local oscillator (LO) for coherent detection. During the generation of the LO lightwave, the carrier and the upper sideband are successfully suppressed by up to 30 dB and 40 dB respectively. An EDFA is used to boost the LO power, and a BPF is used to suppress ASE noise. On the other hand, the lower branch is used to produce a dual-sideband probe lightwave by MZM2 and RF synthesizer with the carrier suppressed up to 30 dB. The frequency of the synthesizer f_s is scanned from 10.78 to 10.88 GHz with a scanning step of 1 MHz to reconstruct the distributed BGS. Thus, the IF signals carrying Brillouin gain information vary from 780 to 880 MHz. Note that the two RF synthesizers for the generation of probe and LO are synchronized with each other to ensure a stable value of the IF. A variable optical attenuator (VOA) is inserted to control the power of each sideband, and an isolator is followed to block the counter-propagating pump lightwave. Here an extra Raman amplifier, depicted as the red region of Fig. 3, will be used for the high spatial resolution experiment in Section III-C.

After the interaction with the pump pulses in FUT, the probe lightwave and LO are then injected into a commercial integrated phase- and polarization-diversity coherent receiver (Fujitsu 100G integrated phase- and polarization-diversity coherent receiver). The four output signals from the receiver include in-phase and quadrature-phase components of the beating signals in both orthogonal polarizations and are collected by a four-channel real-time oscilloscope (OSC, Tektronix DSA72004 Digital Serial Analyzer). Before signal collection, an electrical low-pass filter (DC-1.3 GHz) at each channel of OSC is employed to block the unwanted high-frequency components as shown in Fig. 1(b), i.e., only electrical signals at a frequency of IF are collected. These four output signals are processed by DSP algorithms mentioned above to recover the baseband Brillouin sensing signal and extract sensing information. The whole process does not include any averaging and the data acquisition is finished in a real-time manner.

III. Experiment Results and Discussion

A. Results of the Experiment System

In this demonstration, the FUT is a 40.65 km single-mode fiber (SMF) kept under room temperature (~25 °C) except the last 200 m section placed in an oven heated to 40 °C. The duration of the pump pulses is set as 40 ns, corresponding to 4 m spatial resolution. The peak power of pump pulses is controlled to be ~21 dBm, to prevent nonlinear effects such as modulation instability. While the power of each probe sideband is kept at −8 dBm in order to avoid the non-local effect. During the DSP process, the bandwidth of the subsequent digital bandpass filter is set at 80 MHz to further remove the noise in the frequency domain.

Fig. 4(a) plots the measured BGS distribution along the whole FUT by using the recovered Brillouin time-domain traces from our coherent-detection assisted BOTDA without trace averaging, and Fig. 4(b) shows the corresponding BGS distribution around the last ~2 km, in which the heated section can be clearly observed. With the help of Lorentzian curve fitting, the distribution of BFS along the FUT is illustrated in Fig. 5(a). Fig. 5(b) gives the zoom-in view of the BFS distribution around the last 350 m fiber, while Fig. 5(c) shows the zoom-in view of BFS distribution near the location with temperature transition. The BFS uncertainty of the system, defined as the standard deviation of the BFS values around the last 200 m fiber, is calculated to be 1.437 MHz. In the following sections, the BFS uncertainty is calculated by the same way. And the BFS difference between the heated and unheated fiber is found to be 15 MHz, corresponding to a temperature difference of 15 °C, given the BFS temperature coefficient of ~1.04 MHz/°C, which

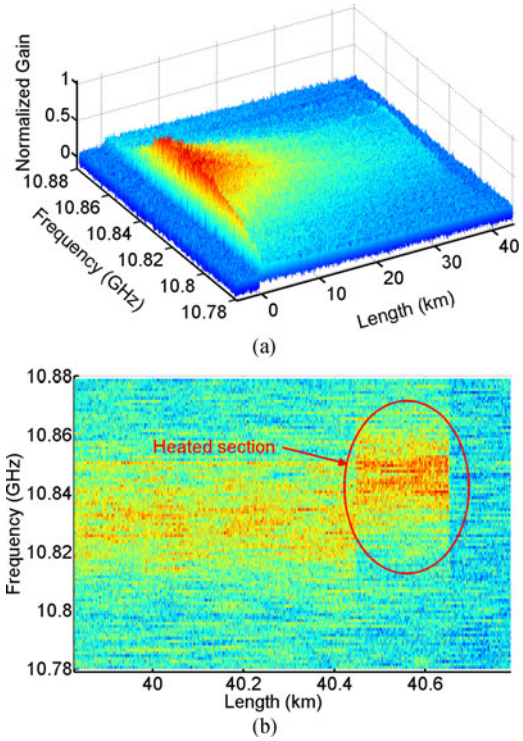

Fig. 4. BGS distribution (a) along the whole FUT and (b) around the last ∼2 km fiber measured by our coherent-detection assisted BOTDA without trace averaging.

well matches our temperature setting. The ∼4 m transition section of in Fig. 5(c) also implies a spatial resolution of ∼4 m, corresponding to 40 ns pump pulse.

B. Enhanced Accuracy by Integrating Image Processing Algorithm Into the System

To further enhance the performance of our proposed coherent BOTDA, we integrate an image denoising algorithm known as non-local means (NLM) [19]–[28] into the DSP process. The experiment parameters are the same as those in Section III-A. There are three parameters in NLM required to optimize according to our configuration: similarity window size, search window and smoothing control parameter *h*. Considering the spatial resolution of 4 m and the sampling interval of 0.32 m, we choose the similarity window size to be 7×7 without sacrifice of the spatial resolution. To reduce the processing time, the search window is set to be 3 times the similarity window, i.e., 21×21. The parameter h is related to the level of denoising and it is set to be 10 times the noise standard deviation, i.e., 0.392. Fig. 6(a) plots the recovered baseband Brillouin time-domain traces at a scanning frequency of 10.83 GHz with (red curve) and without (blue curve) NLM integrated into our coherent BOTDA system, respectively. The trace without NLM is obtained using the results in Section III-A. Fig. 6(b) also shows the comparison between the recovered BGSs at a distance of 40.326 km with and without NLM. We can see that with NLM integrated into our coherent BOTDA system the noise on the recovered signals is greatly suppressed in both space and frequency domain. In Fig. 6(c),

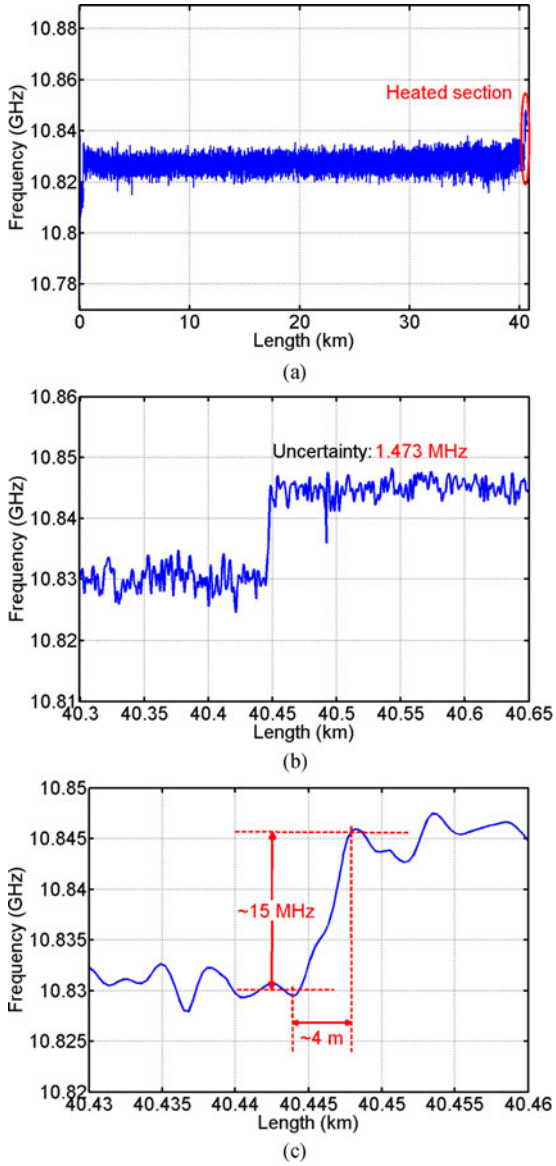

Fig. 5. Measured BFS distribution (a) along the whole FUT, (b) around the last ∼350 m fiber, and (c) around the location with temperature transition.

the BGS distribution after employing the NLM algorithm also shows the good denoising performance.

Similarly, the distribution of the BFS can be obtained using Lorentzian curve fitting, which is given in Fig. 7. It can be seen from Fig. 7 that the fluctuation of the BFS has been reduced significantly with NLM integrated into the system, and hence the BFS uncertainty at the end of the FUT is enhanced from 1.473 MHz to 0.843 MHz. Since the image processing algorithm would not add much system complexity, it can be easily integrated into our coherent BOTDA to achieve better performance without trace averaging.

C. Enhanced Spatial Resolution by Adding a Raman Amplifier

To demonstrate better spatial resolution using our coherent BOTDA system without trace averaging, pump pulses with the duration of 20 ns are employed, corresponding to a spatial reso-

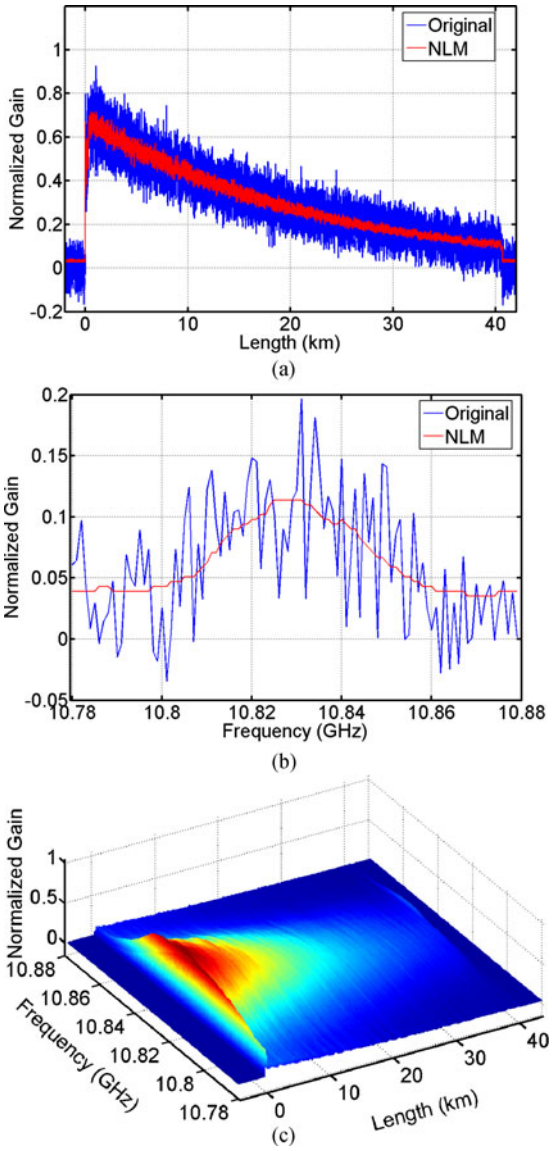

Fig. 6. (a) Recovered baseband Brillouin time-domain traces at a scanning frequency of 10.83 GHz, (b) recovered BGSs at a distance of 40.326 km with (red curve) and without (blue curve) NLM integrated into our coherent BOTDA system, (c) BGS distribution along the whole FUT after using NLM.

lution of 2 m. At the same time, to compensate the degradation of Brillouin gain due to the use of shorter pump pulse, a simple Raman amplifier pumped at 1445 nm is added into the system through a wavelength division multiplexer (WDM), as shown in the red region of Fig. 3. The Raman pump co-propagates with the probe lightwave while counter-propagates with the Brillouin pump pulses in the FUT, where both of them experience distributed Raman amplification. The power of Raman pump laser is kept at 23 dBm to limit the relative intensity noise (RIN) transferred into the amplified lightwaves. On the other hand, the probe power is reduced to −10 dBm in order to avoid the non-local effect. In the DSP process, the bandwidth of subsequent digital bandpass filter is now changed to be 120 MHz to cover broader spectrum at a spatial resolution of 2 m. In this experiment, we use the same FUT as that in Section III-A except 2 m section is put in an ice-water bath (0 °C) and

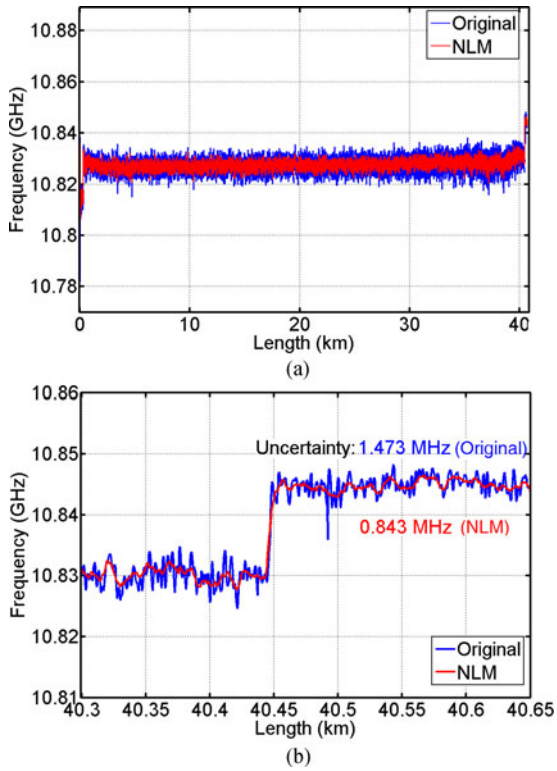

Fig. 7. (a) Recovered baseband Brillouin time-domain traces at a scanning frequency of 10.83 GHz, (b) recovered BGSs at a distance of 40.326 km with (red curve) and without (blue curve) NLM integrated into our coherent BOTDA system.

inserted between the section under room temperature (∼25 °C) and the last 200 m heated section (40 °C). Other experiment parameters are maintained the same as those in Section III-A.

Fig. 8(a) shows the measured BGS distribution around the last ∼350 m section by using the coherent-detection assisted BOTDA without trace averaging, in which three sections at three different temperatures are successfully observed. When further zoomed in, the section in ice water bath is distinguished clearly, as shown in Fig. 8(b). Note that the SNR is improved by 3.3 dB after the Raman amplifictaion is applied in our case.

The BFS distribution along the FUT and the last 350 m fiber are given in Fig. 9(a) and (b). The BFS uncertainty at the end of FUT is calculated to be 2.997 MHz. In Fig. 9(c), the BFS transitions clearly indicate fiber sections under three different temperatures. The BFS difference between the ice-water section and the heated section is ∼40 MHz, corresponding to 40 °C difference in temperature, which matches well with our temperature setting. Moreover, as shown in Fig. 9(c) the 2 m spatial resolution has been achieved and validated from the BFS distribution of the ice-water section.

D. Discussions

The proposed scheme will provide a better power allocation for both the probe and LO lightwaves in terms of coherent detection. In some of previous coherent BOTDA schemes reported in Ref. [14], [15], considering that the two lightwaves propagate together in the FUT, the powers of them are set to be quite

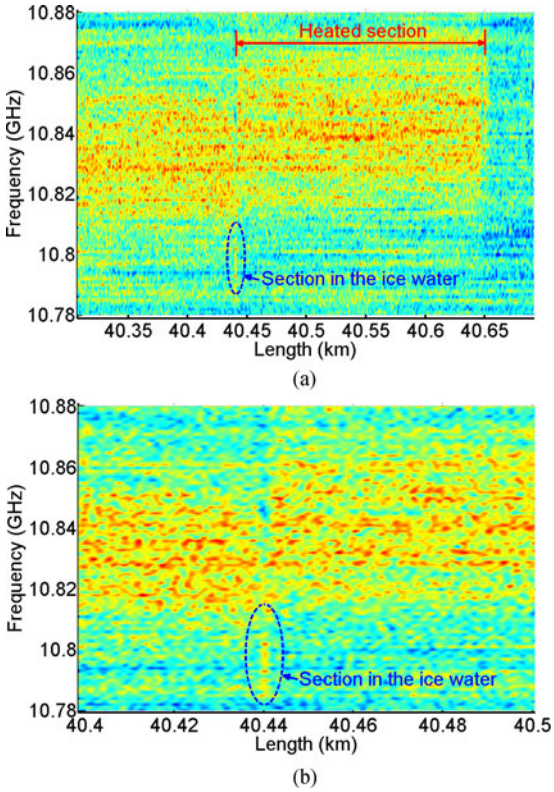

Fig. 8. BGS distribution (a) around the last ~350 m fiber and (b) around the location with two temperature transitions measured by the coherent-detection assisted BOTDA without trace averaging at a spatial resolution of 2 m.

low to avoid fiber nonlinearities. Moreover, the LO lightwave itself will suffer from the fiber attenuation as well, resulting in insufficient power to achieve shot-noise limited sensitivity. In comparison, our proposed scheme will conquer this drawback.

The Figure of Merit (FoM) for the configurations in Sections III-A, III-B, and III-C are calculated to be 18.95, 34.25, and 20.49, respectively. The values seem not attractive compared to some of the reported BOTDA works [4]–[22]. However, the proposed coherent BOTDA scheme does not have trace averaging and sacrifices some sensing performance to pursue the real-time acquisition, which may not be suitably reflected by the value of FoM.

There is a tendency that the DOFS systems based on Brillouin scattering are developed with the feature of fast or dynamic measurement [22]–[26]. Compared to the schemes in Ref. [23]–[26], our proposed scheme has longer sensing range without the need of trace averaging. However, our scheme still requires the time for frequency scanning [23] and the time for frequency switching [24]. The overall measurement time includes the acquisition time and the data processing time. The acquisition time for each scanning frequency mainly consists of the lightwave propagation time (1 ms), the frequency and polarization switching time (200 μs), and the oscilloscope data fetching and saving time (15 s). Due to the fact that our data acquisition is achieved by using oscilloscope and the instrument control system is based on the LabVIEW software, the data fetching and saving time dominates in the data acquisition

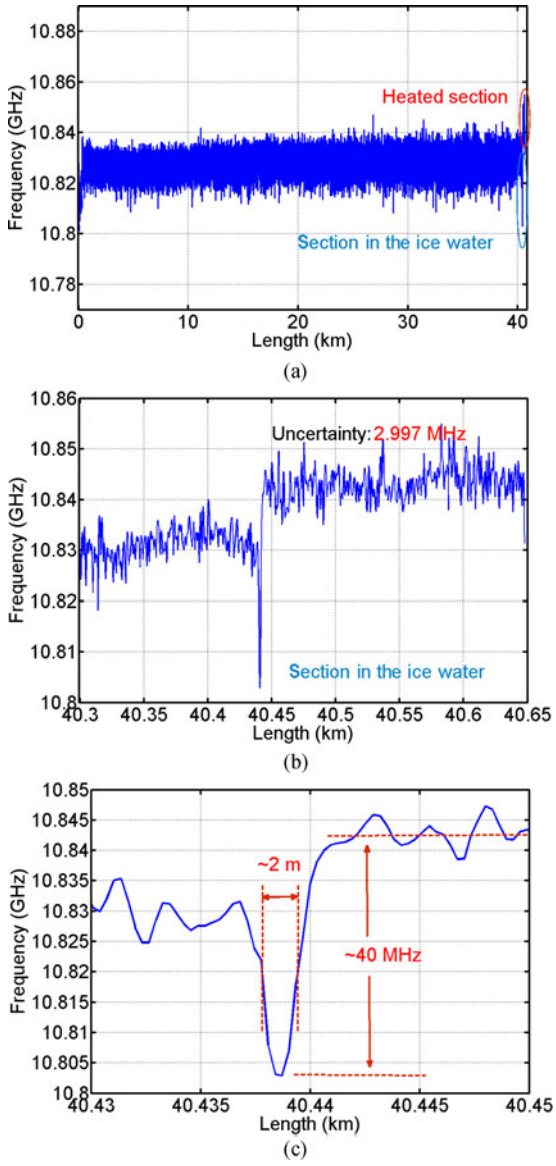

Fig. 9. Measured BFS distribution (a) along the whole FUT, (b) around the last ~350 m fiber, and (c) around the location with temperature transitions.

time. The frequency scanning progress even makes the total acquisition progress longer. For instance, the data acquisition takes about 25 minutes for 100 scanning frequencies. It is still difficult to improve both the spatial resolution and sensing range while maintain fast or dynamic sensing [25], [26]. The other challenge for implementation of fast or dynamic sensing is that the data processing is conducted offline instead of online or in a real-time manner, whose processing time is quite dependent on the computer performance. However, it can be expected that, fast analog-to-digital converter (ADC) and Field Programmable Gate Array (FPGA) techniques shall help the data processing implemented in real time to greatly reduce the processing time.

IV. Conclusion

We have proposed and demonstrated a coherent BOTDA system without trace averaging for distributed temperature

measurement. The LO light for coherent detection is separately generated by modulating the same laser source based on SSB, enabling the enhanced Brillouin signals to be carried on stable IF signals for subsequent extraction using electrical and digital filtering. The IF signals are detected by a commercial integrated phase- and polarization-diversity coherent receiver. Two adjacent Brillouin time-domain traces triggered by two sequential orthogonal polarized pump pulses to minimize polarization dependent fluctuation are recovered using DSP after real-time data acquisition from the four outputs of the coherent receiver without any trace averaging. Benefiting from this configuration, distributed temperature sensing with a spatial resolution of 4 m and BFS uncertainty of 1.473 MHz has been achieved over 40 km sensing range without the need of trace averaging. By integrating appropriately designed NLM algorithm and a simple Raman amplifier into the system, the BFS uncertainty has been further enhanced to 0.843 MHz and the spatial resolution has been improved to 2 m. Thanks to the real-time data acquisition without any trace averaging during the measurement, the configuration is promising for distributed monitoring of temperature/strain in a high-speed manner.

REFERENCES

[1] T. Horiguchi and M. Tateda, "Optical-fiber-attenuation investigation using stimulated Brillouin scattering between a pulse and a continuous wave," *Opt. Lett.*, vol. 14, no. 8, pp. 408–410, Apr. 1989.

[2] T. Horiguchi, K. Shimizu, T. Kurashima, M. Tateda, and Y. Koyamada, "Development of a distributed sensing technique using Brillouin scattering," *J. Lightw. Technol.*, vol. 13, no. 7, pp. 1296–1302, Jul. 1995.

[3] X. Bao and L. Chen, "Recent progress in optical fiber sensors based on Brillouin scattering at university of Ottawa," *Photon. Sens.*, vol. 1, no. 2, pp. 102–117, Jun. 2011.

[4] M. A. Soto and L. Thévenaz, "Modeling and evaluating the performance of Brillouin distributed optical fiber sensors," *Opt. Express*, vol. 21, no. 25, pp. 31347–31366, Dec. 2013.

[5] L. Thévenaz, S. F. Mafang, and J. Lin, "Effect of pulse depletion in a Brillouin optical time-domain analysis system," *Opt. Express*, vol. 21, no. 12, pp. 14017–14035, Jun. 2013.

[6] M. Alem, M. A. Soto, and L. Thévenaz, "Modelling the depletion length induced by modulation instability in distributed optical fibre sensors," in *Proc. SPIE 9157, Int. Conf. Opt. Fiber Sens.*, 2014, Paper 91575S.

[7] A. Dominguez-Lopez, X. Angulo-Vinuesa, A. Lopez-Gil, S. Martin-Lopez, and M. Gonzalez-Herraez, "Non-local effects in dual-probe-sideband Brillouin optical time domain analysis," *Opt. Express*, vol. 23, no. 8, pp. 10341–10352, Apr. 2015.

[8] M. A. Soto, G. Bolognini, F. Di Pasquale, and L. Thévenaz, "Simplex-coded BOTDA fiber sensor with 1 m spatial resolution over a 50 km range," *Opt. Lett.*, vol. 35, no. 2, pp. 259–261, Jan. 2010.

[9] Y. Mao, N. Guo, K. Yu, H. Tam, and C. Lu, "1 Cm spatial resolution Brillouin optical time domain analysis based on bright pulse Brillouin gain and complementary code," *IEEE Photon. J.*, vol. 4, no. 6, pp. 2243–2248, Dec. 2012.

[10] A. Domínguez-López, A. López-Gil, S. Martín-López, and M. González-Herráez, "Signal-to-noise ratio improvement in BOTDA using balanced detection," *IEEE Photon. Technol. Lett.*, vol. 26, no. 4, pp. 338–341, Feb. 2014.

[11] X. Angulo-Vinuesa *et al.*, "Raman assisted Brillouin distributed temperature sensor over 100 km featuring 2 m resolution and 1.2 °C uncertainty," *J. Lightw. Technol.* vol. 30, no. 8, pp. 1060–1065, Apr. 2012.

[12] M. Taki, Y. Muanenda, I. Toccafondo, A. Signorini, T. Nannipieri, and F. Di Pasquale, "Optimized hybrid Raman/fast-BOTDA sensor for temperature and strain measurements in large infrastructures," *IEEE Sens. J.*, vol. 14, no. 12, pp. 4297–4304, Dec. 2014.

[13] M. A. Soto *et al.*, "Extending the real remoteness of long-range Brillouin optical time-domain fiber analyzers," *J. Lightw. Technol.*, vol. 32, no. 1, pp. 152–162, Jan. 2014.

[14] A. Zornoza, M. Sagues, and A. Loayssa, "Self-heterodyne detection for SNR improvement and distributed phase-shift measurements in BOTDA," *J. Lightw. Technol.*, vol. 30, no. 8, pp. 1066–1072, Apr. 2012.

[15] Z. Li, L. Yan, L. Shao, W. Pan, and B. Luo, "Coherent BOTDA sensor with intensity modulated local light and IQ demodulation," *Opt. Express*, vol. 23, no. 12, pp. 16407–16415, Jun. 2015.

[16] Z. Li *et al.*, "Precise Brillouin gain and phase spectra measurements in coherent BOTDA sensor with phase fluctuation cancellation," *Opt. Express*, vol. 24, no. 5, pp. 4824–4833, Mar. 2016.

[17] L. Wang *et al.*, "Coherent BOTDA using phase- and polarization-diversity heterodyne detection and embedded digital signal processing," *IEEE Sens. J.*, vol. 17, no. 12, pp. 3728–3734, Jun. 2017.

[18] N. Guo *et al.*, "Bi-directional Brillouin optical time domain analyzer system for long range distributed sensing," *Sensors* vol. 16, no. 12, Dec. 2016, Art. no. 2156.

[19] M. A. Soto, J. A. Ramírez, and L. Thévenaz, "Intensifying the response of distributed optical fibre sensors using 2D and 3D image restoration," *Nature Commun.*, vol. 7, Mar. 2016, Art. no. 10870.

[20] Y. Dong, L. Chen, and X. Bao, "Extending the sensing range of Brillouin optical time-domain analysis combining frequency-division multiplexing and in-line EDFAs," *J. Lightw. Technol.*, vol. 30, no. 8, pp. 1161–1167, Apr. 2012.

[21] Y. Dong, H. Zhang, L. Chen, and X. Bao, "2 cm spatial-resolution and 2 km range Brillouin optical fiber sensor using a transient differential pulse pair," *Appl. Opt.*, vol. 51, no. 9, pp. 1229–1235, Mar. 2012.

[22] A. Dominguez-Lopez *et al.*, "Resolving 1 million sensing points in an optimized differential time-domain Brillouin sensor," *Opt. Lett.*, vol. 42, no. 10, pp. 1903–1906, May 2017.

[23] A. Voskoboinik *et al.*, "Sweep-free distributed Brillouin time-domain analyzer (SF-BOTDA)," *Opt. Express*, vol. 19, no. 26, pp. B842–B847, Dec. 2011.

[24] Y. Peled, A. Motil, and M. Tur, "Fast Brillouin optical time domain analysis for dynamic sensing," *Opt. Express*, vol. 20, no. 8, pp. 8584–8591, Apr. 2012.

[25] J. Fang, W. Shieh, and P. Xu, "Single-shot Brillouin optical time domain analysis for distributed fiber sensing," in *Proc. IEEE Conf. Sens.*, 2016, pp. 1–3.

[26] C. Jin *et al.*, "Single-measurement digital optical frequency comb based phase-detection Brillouin optical time domain analyzer," *Opt. Express*, vol. 25, no. 8, pp. 9213–3224, Apr. 2017.

[27] N. Guo *et al.*, "Coherent-detection-assisted BOTDA system without averaging using single-sideband modulated local oscillator signal," in *Proc. SPIE 10323, Int. Conf. Opt. Fiber Sens.*, 2017, Paper 103237L.

[28] A. Buades, B. Coll, and J. M. Morel, "A non-local algorithm for image denoising," in *Proc. IEEE Comput. Soc. Conf. Comput. Vis. Pattern Recog.*, vol. 2, 2005, pp. 60–65.

Nan Guo received the B.Eng. degree in automation from Nanjing University, Nanjing, China, in 2011. In September 2013, he started working toward the Ph.D. degree at the Hong Kong Polytechnic University, Kowloon, Hong Kong. He joined Prof. Chao Lu's research group at the Hong Kong Polytechnic University as a Research Assistant in 2011. His research focuses on the distributed optical fiber sensing system based on Brillouin scattering.

Liang Wang received the B.S. degree from the Huazhong University of Science and Technology, Wuhan, China, in 2008, and the Ph.D. degree from The Chinese University of Hong Kong (CUHK), Shatin, Hong Kong, in 2013. He is currently an Assistant Professor (Research) in the Department of Electronic Engineering, CUHK. From September 2013 to January 2014, he worked as a Research Scientist (core staff) in the Institute for Infocomm Research, A∗STAR, Singapore. In February 2014, he as a Postdoctoral Fellow joined the Photonics Research Center, The Hong Kong Polytechnic University, where he received The Hong Kong Polytechnic University Postdoctoral Fellowships. In September 2016, he joined the CUHK as an Assistant Professor. He has published more than 70 research papers in major peer-reviewed journals and international conferences. His research interests include fiber sensors, optical signal processing for optical communications, novel fiber devices and photonic devices, etc.

Huan Wu is currently working toward the Ph.D. degree in the Department of Electronic Engineering, The Chinese University of Hong Kong, Shatin, Hong Kong.

Chao Jin received the B.Eng. degree in electronics engineering from Shandong University, Jinan, China, in 2010. He worked toward the Master's degree at Jinan University, Guangzhou, China, from 2011 to 2014. He started working toward the Ph.D. degree at The Hong Kong Polytechnic University, Kowloon, Hong Kong, from 2015. In 2013, he worked as a Research Assistant in Prof. Chao Lu's group. His research interests include the distributed optical fiber sensing and optical telecommunication.

Hwa-Yaw Tam received the B.Sc. and Ph.D. degrees in electrical and electronic engineering from the University of Manchester, Manchester, U.K.

From 1989 to 1993, he was with Hirst Research Center, GEC-Marconi Ltd., London and worked on WDM optical components and systems, and erbium optical fiber amplifiers. He conducted pioneering works in optical fiber amplifiers, invented and patented the low-loss splicing technique for erbium-doped fibers, which enhanced the performance of optical amplifiers significantly. In 1992, he built two of the first batch of optical amplifiers for Italian PTT. He joined The Hong Kong Polytechnic, Kowloon, Hong Kong, in 1993 and currently is the Department Head and the Chair Professor of photonics in the Department of Electrical Engineering, and the Director of the Photonic Research Centre, The Hong Kong Polytechnic University. He established several world-class research facilities at PolyU, including two fiber-drawing towers for fabrication of photonics crystal fibers and polymer optical fibers, an Ultrahigh Speed Communication Laboratory, and laser platforms for the fabrication of advanced fiber gratings. He has strong R&D collaboration with the industry and his team installed many FBG sensing systems, including an FBG-based SHM system for the 610-m Canton Tower in Guangzhou, China, and several condition-monitoring systems for railways in Hong Kong, China mainland, Taiwan, and India. Currently, his R&D team is building the world's first city-wide fiber-optic sensing network for condition-based monitoring of metro systems in Hong Kong. He has published more than 500 technical papers and awarded/applied about 20 patents, has extensive international research collaborations with many universities around the world, and is a Keynote/Invited Speaker at more than 40 international conferences. His current research interests include fabrication of specialty optical silica fibers and polymer fibers, optical fiber communications, and fiber sensor systems based on fiber Bragg gratings and photonic crystal fibers. He received numerous international awards for his inventions, and is the Third Prize Winner of the Berthold Leibinger Innovationspreis 2014. Berthold Leibinger Innovationspreis is a biennial event and it is one of the highest remunerated international innovation prizes for laser technology. He is a Fellow of the Optical Society of America.

Chao Lu received the B.Eng. degree in electronic engineering from Tsinghua University, Beijing, China, in 1985, and the M.Sc. and Ph.D. degrees from the University of Manchester, Manchester, U.K., in 1987 and 1990, respectively.

After graduation, he joined the School of Electrical and Electronic Engineering, Nanyang Technological University, Singapore, as a Lecturer in 1991. In January 1999, he continued his work as an Associate Professor. From June 2002 to December 2005, he was seconded to the Institute for Infocomm Research, Agency for Science, Technology and Research (A∗STAR), Singapore, as the Program Director and the Department Manager, helping to establish a research group in the area of optical communication and fiber devices. Since April 2006, he has been a Professor in the Department of Electronic and Information Engineering, the Hong Kong Polytechnic University, Kowloon, Hong Kong. His research interests include optical communication systems and networks, fiber devices for optical communication, and sensor systems. In 2017, he became an OSA Fellow.